ELSEVIER

Physica B 244 (1998) 60–65

PHYSICA B

Infrared spectroscopy on $Y_{1-x}RE_xBa_2Cu_{3-y}Zn_yO_6$ (RE = Pr, Gd, $x = 0$ and 0.8; $y = 0$ and ≈ 0.15)

M. Grüninger[a,*], D. van der Marel[a], H.P. Geserich[b], Th. Wolf[c], A. Erb[d], T. Kopp[e]

[a] *Laboratory of Solid State Physics, Materials Science Center, University of Groningen, 9747 AG Groningen, The Netherlands*
[b] *AP, University of Karlsruhe, Germany*
[c] *ITP, Forschungszentrum Karlsruhe, Germany*
[d] *DPMC, University of Geneva, Switzerland*
[e] *TKM, University of Karlsruhe, Germany*

Abstract

Far- and mid-infrared properties of antiferromagnetic $Y_{1-x}RE_xBa_2Cu_{3-y}Zn_yO_6$ (RE = Pr, Gd, $x = 0$ and 0.8; $y = 0$ and ≈ 0.15) were investigated by infrared reflection and transmission measurements ($\boldsymbol{k} \| c$-axis). All six phonon modes of E_u symmetry and several multi-phonon bands were observed. Zn substitution causes phonon side bands and a surprising temperature dependence of multi-phonon bands, possibly due to spin-lattice interactions. All compounds show several features in the mid-infrared range that might be related to bimagnon-plus-phonon absorption. Published by Elsevier Science B.V.

Keywords: Antiferromagnetic cuprates; Multi-phonons; Magnons; Zn substitution; $YBa_2Cu_3O_6$; Far-infrared spectroscopy

1. Introduction

All cuprate high-T_c superconductors show also insulating, antiferromagnetic phases. Due to the high resolution and the wide frequency range, infrared spectroscopy is an excellent tool to observe the various low-energy excitations in these so-called parent compounds. In addition to phonon features, it is also possible to study, for instance, magnetic excitations such as the bimagnon-plus-phonons recently described in La_2CuO_4 [1, 2]. In this paper, we study the influence of rare earth and Zn substitution on (multi-)phonon and bimagnon-plus-phonon absorption.

* Corresponding author. Tel.: +31 50 363 4812; fax: +31 50 363 4825; e-mail: markus@phys.rug.nl.

0921-4526/98/$19.00 Published by Elsevier Science B.V.
PII S0921-4526(97)00462-6

2. Experimental

Single crystals of $RE_xY_{1-x}Ba_2Cu_3O_6$ (RE = Pr, Gd; $x = 0$ and 0.8) were grown in Y_2O_3 stabilized ZrO_2 crucibles as described elsewhere [3]. In the case of $YBa_2Cu_{3-y}Zn_yO_6$ [4], the melt nominally contained 5% of Zn, and hence we obtain $0.1 \leqslant y \leqslant 0.2$. The samples had typical dimensions of 1×1 mm^2 in the *ab*-plane. For the transmission measurements the samples need to be thin in the *c*-direction. The Zn-free crystals were 68 and 50 μm ($YBCO_6$), 126 μm ($PrYBCO_6$) and 231 μm ($GdYBCO_6$) thick, whereas the $YBa(CuZn)O_6$ sample was polished down to 35 μm. The samples were annealed in flowing argon in order to exclude doping by excess oxygen. The reflection and transmission measurements were performed in two

different laboratories using two Bruker 113v Fourier spectrometers in the spectral range from 6 meV to 1 eV. All measurements were carried out with $\boldsymbol{k} \| c$ and the electric field vector parallel to the *ab*-plane. The samples were mounted on a diaphragm in a He-flow cryostat that allowed for measurements in the temperature range from 4 to 485 K. The transmission (reflection) measurements were calibrated against the same diaphragm (using a gold mirror as a reference).

3. Results

3.1. Far-infrared

The reflectivity of $YBa(CuZn)O_6$ at $T = 4$ K is plotted in the upper panel of Fig. 1. The spectrum of the optical conductivity $\sigma_1(\omega)$ shown in the lower panel was obtained by a Lorentz fit of the reflectivity data. At first sight, the spectrum is typical for an insulator and shows five of the six phonons of E_u symmetry. As the sample is only 35 μm thick, we observe interference fringes in the frequency ranges of low absorption, i.e. below 100 cm^{-1} and between the phonons. Here, we want to concentrate on the phonon peaks at 115 and 600 cm^{-1}, as these show

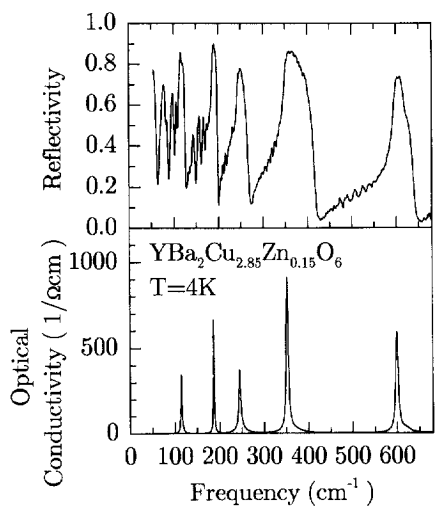

Fig. 1. Upper panel: Reflectivity of a thin single crystalline platelet ($d = 35$ μm) of $YBa(CuZn)O_6$ for $E \| ab$ at $T = 4$ K. Lower panel: $\sigma_1(\omega)$ as obtained from a Lorentz fit.

structures that are induced by Zn impurities: the phonon side bands at 121 and at 608 cm^{-1}. The temperature dependence of these features is plotted on a larger scale in Fig. 2. In $\sigma_1(\omega)$ these side bands give rise to an asymmetric line shape, showing up in the tails. The peak at 600 cm^{-1} corresponds to an in plane Cu–O–Cu bond stretching mode. This mode is extremely sensitive to the Cu–O distance [5, 6], as can be seen from the strong temperature dependence of the eigenfrequency, and hence it is plausible that Zn impurities give rise to a side peak. The broad shoulder at about 625 cm^{-1} is present also in Zn-free $YBCO_6$ and will be discussed in more detail in a forthcoming paper [7]. The peak at 115 cm^{-1} seems to be the lowest phonon mode and has therefore been interpreted as a Ba mode by most authors, usually arguing that the Ba mode should be the lowest one, as Ba is the heaviest ion in

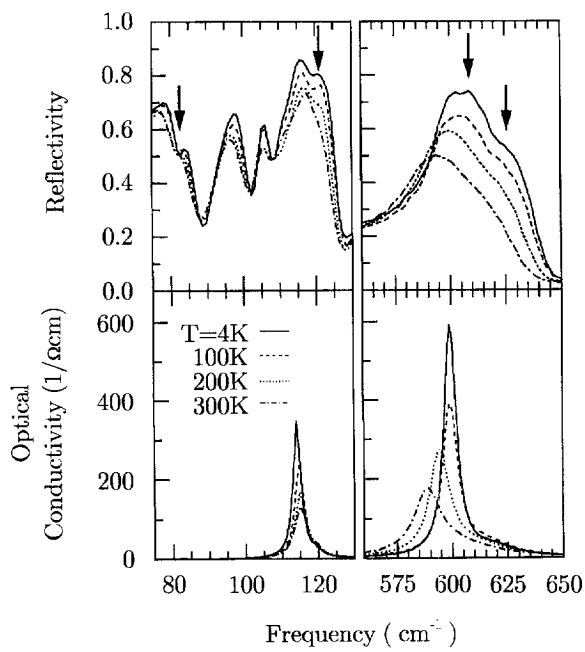

Fig. 2. Enlarged plot for two phonons of $R(\omega)$ and $\sigma_1(\omega)$ of a thin single crystalline platelet ($d = 35$ μm) of $YBa(CuZn)O_6$ for $E \| ab$ at $T = 4$ (solid line), 100 (dashed), 200 (dotted) and 300 K (dashed–dotted). Upper left panel: Left arrow: sixth phonon of E_u symmetry. Right arrow: side peak of the Cu(1) phonon mode induced by Zn impurities. Upper right panel: Left arrow: side peak of the in plane Cu–O–Cu stretching mode induced by Zn impurities. Right arrow: shoulder present in all samples, not related to the Zn impurities.

the system. However, the weakly infrared active sixth phonon of E_u symmetry was found at a still lower frequency of 83 cm^{-1} in the far-infrared transmission spectrum of $YBCO_6$ [8]. In the reflectivity data it can be identified with the dip in the interference pattern at 83 cm^{-1} (see left arrow in Fig. 2). Weak absorption causes a dip in an interference maximum and a peak in a minimum. The observation of a lower mode at 83 cm^{-1} presents a new candidate for the Ba mode. This assignment is supported by lattice dynamical calculations [9], which show only a small oscillator strength for the Ba mode. In this case, the phonon peak at 115 cm^{-1} originates from the motion of the copper ions on the Cu(1) site (the 'chain' site in $YBCO_7$) [10]. The side band at 121 cm^{-1} can thus be understood easily if we assume that some of the substituted Zn ions occupy the Cu(1) sites.

3.2. Mid-infrared

Phonons are the only absorption processes below the charge transfer gap at 1.6 eV that are strong enough to be observed in reflectivity measurements of the antiferromagnetic cuprates. However, in the transmission spectra of thin single crystalline platelets many other interesting features can be found. Fig. 3 shows mid-infrared transmission data of $YBa(CuZn)O_6$, $PrYBCO_6$ and $GdYBCO_6$ in the frequency range above the phonons. All the three spectra show a very rich structure. The differences in absolute value are mainly due to the differences

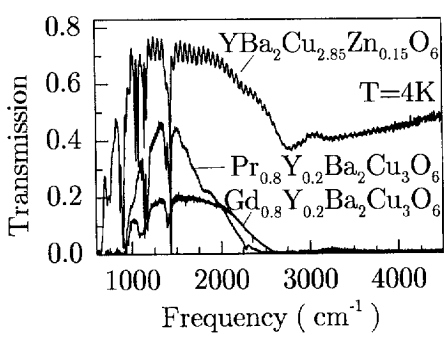

Fig. 3. MIR transmission of single crystals of $YBa(CuZn)O_6$ ($d = 35$ μm), $PrYBCO_6$ ($d = 126$ μm) and $GdYBCO_6$ ($d = 231$ μm) for $E\|ab$ at $T = 4$ K.

in thickness. As we measured both transmission and reflection, it is now possible to calculate $\sigma_1(\omega)$ directly. The temperature dependence of $\sigma_1(\omega)$ is plotted in Fig. 4. The upper panel shows $\sigma_1(\omega)$ of $YBCO_6$ as a reference for the substituted samples. The absolute value of $\sigma_1(\omega)$ is quite similar for all four compounds. They are all very close to the antiferromagnetic limit, $\sigma_1(\omega)$ is about two to three (five) orders of magnitude smaller than in $YBCO_{6.1}$ ($YBCO_7$). Also the basic features are quite similar for the four compounds. Below 1200 cm^{-1} we can observe some multi-phonon bands (the upper limit

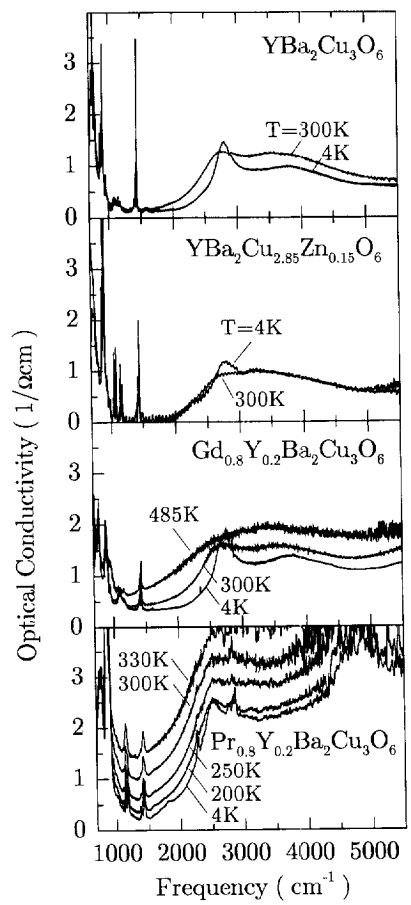

Fig. 4. MIR $\sigma_1(\omega)$ of $YBCO_6$, $YBa(CuZn)O_6$, $PrYBCO_6$ and $GdYBCO_6$ for $E\|ab$ as calculated from $T(\omega)$ and $R(\omega)$. The remnants of interference fringes (e.g. for Zn) are due to the finite opening angle of the light beam and the different incident angles for $R(\omega)$ and $T(\omega)$ (R cannot be measured at absolute normal incidence).

for two-phonon absorption is at about 1350 cm^{-1}), to which we will come back later. Most features at higher energies have a magnetic origin. One exception is the sharp peak at 2275 cm^{-1} in $PrYBCO_6$, which recently has been assigned to an intermultiplet transition in the Pr^{3+} ion [11]. The temperature dependence of this absorption feature shows clear evidence of an interaction between Cu and Pr spins [11].

Common to all four compounds are the sharp peak at about 1436 cm^{-1}, the broad feature at about 2800 cm^{-1} and a second broad peak at higher energies. Some of us had assigned these three peaks to direct magnon absorption [12], which can be weakly allowed by spin–orbit coupling. In this scenario, the feature at 1436 cm^{-1} was explained as absorption of a single magnon of the optical branch. However, recent neutron scattering experiments on $YBCO_x$ ($x = 6.2$ [13] and $x = 6.15$ [14]) show that the optical magnon branch has an energy of about 520 cm^{-1} at $\boldsymbol{k} = 0$, which means that we need an alternative explanation. A peak similar to the one at 2800 cm^{-1} was found in single-layer cuprates as well [1] and has been described successfully as bimagnon-plus-phonon absorption [2]. The term bimagnon denotes a bound state of two magnons, and the combination with a phonon is necessary because a bimagnon does not have a dynamic dipole moment due to the inversion symmetry between spins on adjacent copper sites. Besides the above mentioned case of the $S = \frac{1}{2}$, 2D cuprates, this bimagnon-plus-phonon approach has also been used to describe absorption features in La_2NiO_4 ($S = 1$, 2D) [15, 16] and Sr_2CuO_3 ($S = \frac{1}{2}$, 1D) [17, 18]. The application of this scenario to the bilayer cuprates will be given in a forthcoming paper [6].

Here, we only want to treat the dependence of the peak energies on substitution and the temperature dependence. The peak values at $T = 4$ K are summarized in Table 1. All three peaks shift to lower energies on rare earth or Zn substitution (in the Zn and the Pr substituted samples it is not possible to determine the position of the highest peak). This redshift has to be explained by either a redshift of the phonon part or a decrease of the exchange coupling constants J (in-plane) and/or J_{12} (intra-bilayer). In the case of Zn, the phonon energies hardly change and the shifts have to be due to a softening of the exchange constants caused by the non-magnetic Zn impurities. These will also give rise to some broadening, which indeed is observed. The broadening might be the reason why we do not see a clear peak at about 3800 cm^{-1} any more. In the case of the rare earths, the increase in the lattice parameter a due to the larger radius of the rare-earth ions will influence both the phonon frequencies and the exchange constants. Some broadening could arise from the disorder caused by the 20% of Y on the rare-earth site. This disorder splits the peak at 2795 cm^{-1} for both the Gd and the Pr substituted samples, which both show – besides the redshifted main peak – remnants of the feature of pure $YBCO_6$. Regarding the temperature dependence, it is interesting to note that the peak at about 2800 cm^{-1} is more sensitive to an increase in temperature than the other two peaks of interest here. This is evident from the 485 K data of $GdYBCO_6$ and also from the 300 K curve of $YBa(CuZn)O_6$. The stronger temperature dependence of $YBa(CuZn)O_6$ is probably related to the lower Néel temperature, which is about 500 K [19] for $YBCO_6$ and which we estimate to be a little bit higher than 300 K [20] for $YBaCu_{2.85}Zn_{0.15}O_6$ from our data.

Table 1
Peak frequencies ($T = 4$ K) of the most prominent MIR excitations

$YBCO_6$	1436.2	2795	3780
$YBa(CuZn)O_6$	1435.5	2775	(3260)
$GdYBCO_6$	1434.8	2725	3750
$PrYBCO_6$	1432.7	2520	

Now, we want to focus on the multi-phonon range below 1200 cm^{-1} (see Fig. 5). The detailed shape of the multi-phonon peaks is strongly sample dependent [12, 6], but we find three main bands at about 700–800 cm^{-1}, 850–950 cm^{-1} and 1050–1200 cm^{-1} in all samples. The most probable contributions to these bands are combinations of two oxygen bending modes, of an O bending and an O stretching mode and of two O stretching modes, respectively. The lowest band could also be due to a combination of an O stretching and a rare-earth mode. The strong sample dependence

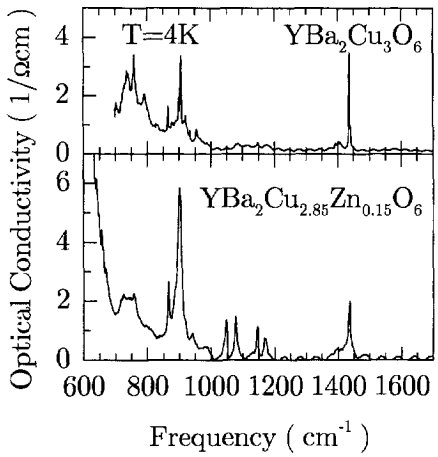

Fig. 5. Comparison of the multi-phonon features below 1200 cm^{-1} in $YBCO_6$ and $YBa(CuZn)O_6$.

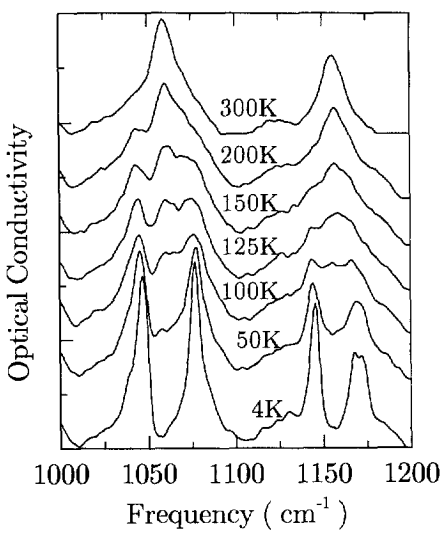

Fig. 6. Temperature dependence of multi-phonon peaks in $YBa(CuZn)O_6$. Note that spectra at intermediate temperatures (100 and 125 K) contain the structures of both high- and low-temperature spectra at the same time.

of the exact shape of the three bands leads us to the conclusion that most of these absorption features are forbidden and only weakly allowed due to the presence of some impurities. A comparison of the strength of the multi-phonon absorption in $YBCO_6$ and $YBa(CuZn)O_6$ supports this view, as the spectral weight of especially the second and third band

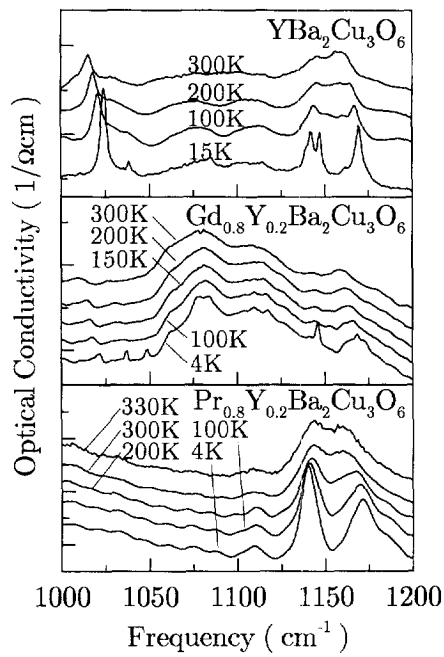

Fig. 7. Same as Fig. 6 for the other three samples. Contrary to $YBa(CuZn)O_6$, all three samples show two separate peaks at about 1150 cm^{-1} for all temperatures presented here.

increases considerably by Zn substitution. A similar increase in the spectral weight of multi-phonons was observed upon substitution of several percent of Cu by Co [21].

But, Zn impurities also give rise to a surprising temperature dependence of the multi-phonon band between 1050 and 1200 cm^{-1} (see Fig. 6 for $YBa(CuZn)O_6$ and Fig. 7 for the three other samples). In $YBa(CuZn)O_6$ this band at $T = 300$ K consists of two main peaks at about 1060 and 1155 cm^{-1}, both of which split at lower temperatures. However, at intermediate temperatures (125 K (100 K) for the peak at 1060 cm^{-1} (1155)) we observe a *superposition* of the 300 K and the 4 K data. The spectra of the other three samples show the same splitting at about 1150 cm^{-1} at low temperature, but the peaks remain split at all temperatures presented here. However, the 200 and 300 K $YBCO_6$ curves resemble the 100 and 125 K $YBa(CuZn)O_6$ data. Possibly, this reflects the difference in the Néel temperature, in which case the splitting would be related to spin-lattice

interactions. The features at about 1060 cm^{-1} are unique to $YBa(CuZn)O_6$.

In conclusion, we presented the temperature dependence and the influence of Zn, Pr and Gd substitution on (multi-) phonons and bimagnon-plus-phonons in $YBCO_6$. We find phonon side bands, indications of spin-lattice interactions and a softening of bimagnon-plus-phonon peaks.

References

[1] J.D. Perkins, J.M. Graybeal, M.A. Kastner, R.J. Birgeneau, J.P. Falck, M. Greven, Phys. Rev. Lett. 71 (1993) 1621.

[2] J. Lorenzana, G.A. Sawatzky, Phys. Rev. Lett. 74 (1995) 1867.

[3] A. Erb, T. Traulsen, G. Müller-Vogt, J. Crystal Growth 137 (1994) 487.

[4] Th. Wolf, W. Goldacker, B. Obst, G. Roth, R. Flükiger, J. Crystal Growth 96 (1989) 1010.

[5] S. Tajima, T. Ido, S. Ishibashi, T. Itoh, H. Eisaki, Y. Mizuo, T. Arima, H. Takagi, S. Uchida, Phys. Rev. B 43 (1991) 10496.

[6] W. Reichardt, N. Pyka, L. Pintschovius, B. Hennion, G. Collin, Physica C 162–164 (1989) 464.

[7] M. Grüninger, D. van der Marel, A. Erb, T. Kopp, to be published.

[8] M. Grüninger, D. van der Marel, P.J.M. van Bentum, A. Erb, H.P. Geserich, T. Kopp, J. Low Temp. Phys. 105 (1996) 389.

[9] C. Thomsen, M. Cardona, W. Kress, R. Liu, L. Genzel, M. Bauer, E. Schönherr, U. Schröder, Solid State Commun. 65 (1988) 1139.

[10] M. Bauer, I.B. Ferreira, L. Genzel, M. Cardona, P. Murugaraj, J. Maier, Solid State Commun. 72 (1989) 551.

[11] A. Zibold, H.L. Liu, D.B. Tanner, J.Y. Wang, M. Grüninger, H.P. Geserich, T. Kopp, Th. Wolf, W. Widder, H.F. Braun, Phys. Rev. B 55 (1997) 11096.

[12] M. Grüninger, J. Münzel, A. Gaymann, A. Zibold, H.P. Geserich, T. Kopp, Europhys. Lett. 35 (1996) 55.

[13] D. Reznik, P. Bourges, H.F. Fong, L.P. Regnault, J. Bossy, C. Vettier, D.L. Milius, I.A. Aksay, B. Keimer, Phys. Rev. B 53 (1996) R14741.

[14] S.M. Hayden, G. Aeppli, T.G. Perring, H.A. Mook, F. Doğan, Phys. Rev. B 54 (1996) R6905.

[15] J.D. Perkins, D.S. Kleinberg, M.A. Kastner, R.J. Birgeneau, Y. Endoh, K. Yamada, S. Hosoya, Phys. Rev. B 52 (1995) R9863.

[16] J. Lorenzana, G.A. Sawatzky, Phys. Rev. B 52 (1995) 9576.

[17] H. Suzuura, H. Yasuhara, A. Furusaki, N. Nagaosa, Y. Tokura, Phys. Rev. Lett. 76 (1996) 2579.

[18] J. Lorenzana, R. Eder, Phys. Rev. B 55 (1997) R3358.

[19] J.M. Tranquada, D.E. Cox, W. Kunnmann, H. Moudden, G. Shirane, M. Suenaga, P. Zolliker, D. Vaknin, S.K. Sinha, M.S. Alvarez, A.J. Jacobson, D.C. Johnston, Phys. Rev. Lett. 60 (1988) 156.

[20] P. Bourges, Y. Sidis, B. Hennion, R. Villeneuve, G. Collin, J.F. Marucco, Physica C 235–240 (1994) 1683.

[21] A. Zibold, D.B. Tanner, Th. Wolf, Bull. APS 42 (1997) 237.